EUROPEAN ORGANISATION FOR NUCLEAR RESEARCH

CERN/SPSLC 94-25
SPSLC P282
October 10, 1994

Proposal

Neutron halo and antiproton - nucleus potential from antiprotonic X-rays

J. Jastrzębski*, M. Kisieliński, P. Lubiński, L. Pieńkowski, A. Trzcińska
Heavy Ion Laboratory, Warsaw University, PL-02-097 Warsaw, Poland

J. Skalski, R. Smolańczuk, S. Wycech
Soltan Institute for Nuclear Studies, PL-00-681, Warsaw, Poland

K. Gulda, W. Kurcewicz*
Institute of Experimental Physics, Warsaw University, PL-00-681, Warsaw, Poland

T. von Egidy, F.J. Hartmann, S. Schmid, W. Schmid
Physik Department, Technische Universität München, D-85747 Garching, Germany

ABSTRACT

It is proposed to investigate the characteristics of antiprotonic X-rays in a number of heavy nuclei. The objective of this study is a combined analysis of observables depending on the nuclear periphery and the antiproton-nucleus optical potential. These observables would be gathered during the realisation of the proposed program (X-rays level shifts and widths) and will also come from the previous neutron halo investigation performed within the PS203 experiment. The present Proposal demonstrates that such an analysis will substantially improve our knowledge of the nuclear periphery in heavy nuclei and, at the same time, will substantially delimitate the parameters defining the antiproton-nucleus optical potential. In 1995 we request 3 weeks of the beam time for this experiment (about 10^5 $\overline{p}$/s, 200 MeV/c).

* Presently at CERN, PPE Division, Isolde Group

Nuclear surface study

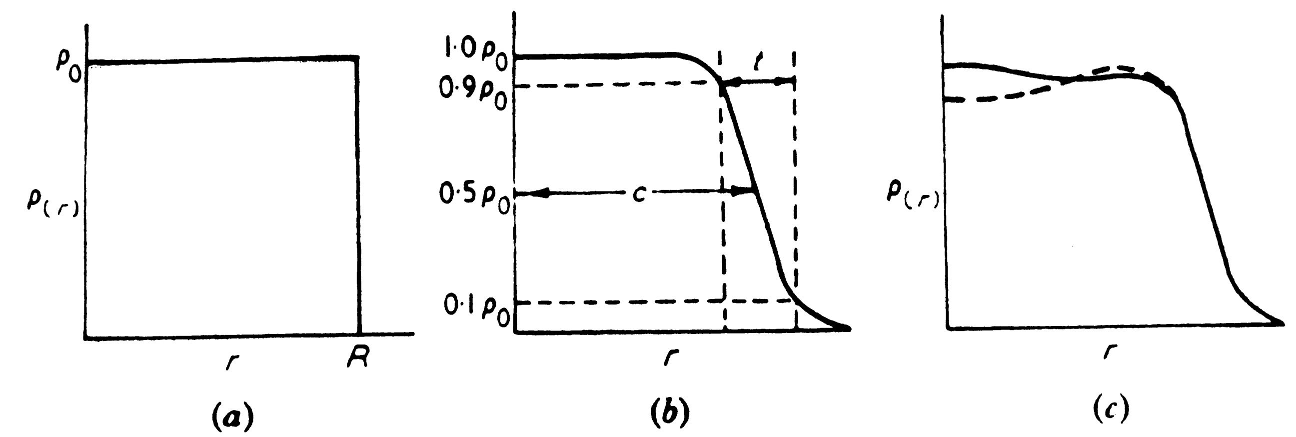

Figure 1. Examples of nuclear matter distributions. (*a*) Billiard ball nucleus with a well-defined radius *R*. (*b*) The fermi distribution. (*c*) Shell model distribution.

$$A \rho_m(r) = Z \rho_p(r) + N \rho_n(r)$$

Fermi $$\rho = \rho_0 \left[1 + \exp(r-c)/a \right]^{-1}$$

$$t = 4.4\, a$$

$$\langle r^2 \rangle = \int_0^\infty r^2 \rho(r) \cdot 4\pi r^2 \, dr$$

1 fm skin expected

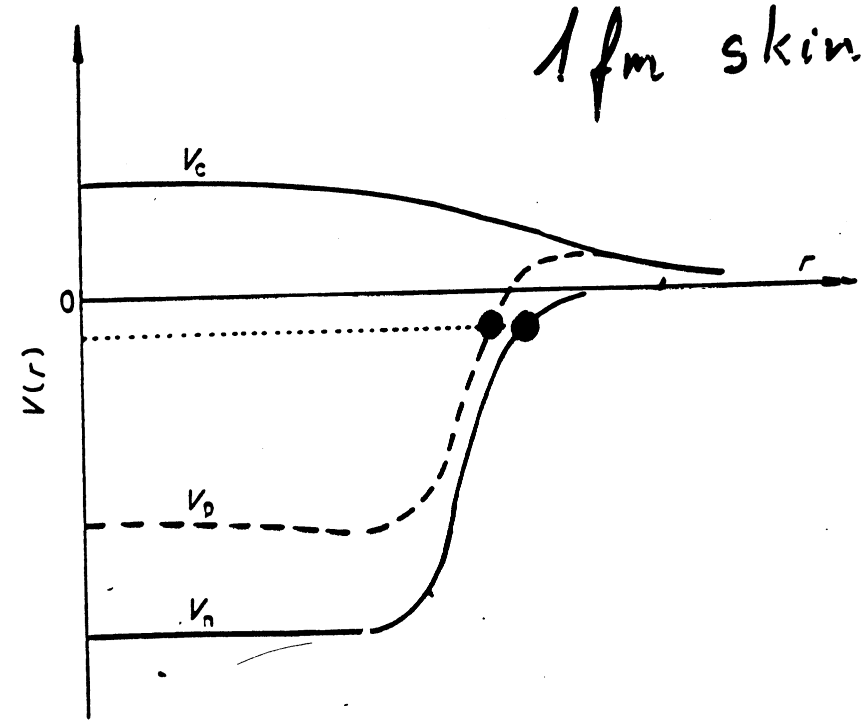

Figure 2. Behaviour of neutron and proton potentials on the assumption that $V_p = V_n + V_c$.

M. H. Johnson and E. Teller

Phys. Rev. 93, 357 (1954)

however $|V_p| > |V_n|$

Is the Surface of the Nucleus Neutron-Rich?

D. H. Wilkinson
(1967)

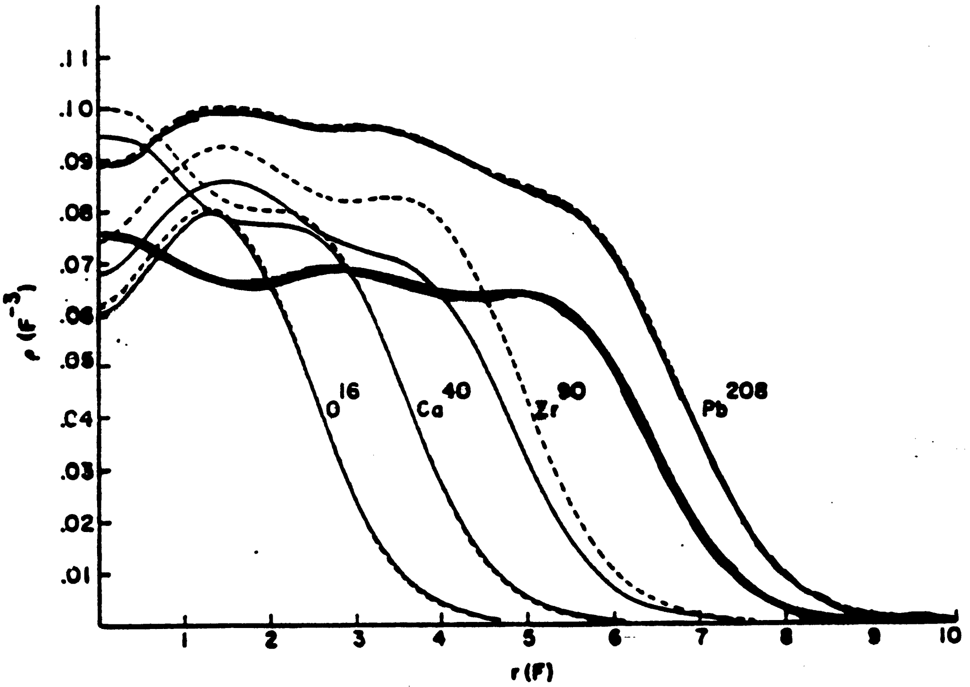

FIG. 1. Neutron (dashed lines) and proton (solid lines) density distributions, with no nucleon size or c.m. motion corrections.

J. W. Negele   Phys. Rev. C1, 1260 (1970

For Pb $r_n^{rms} > r_p^{rms}$

4%

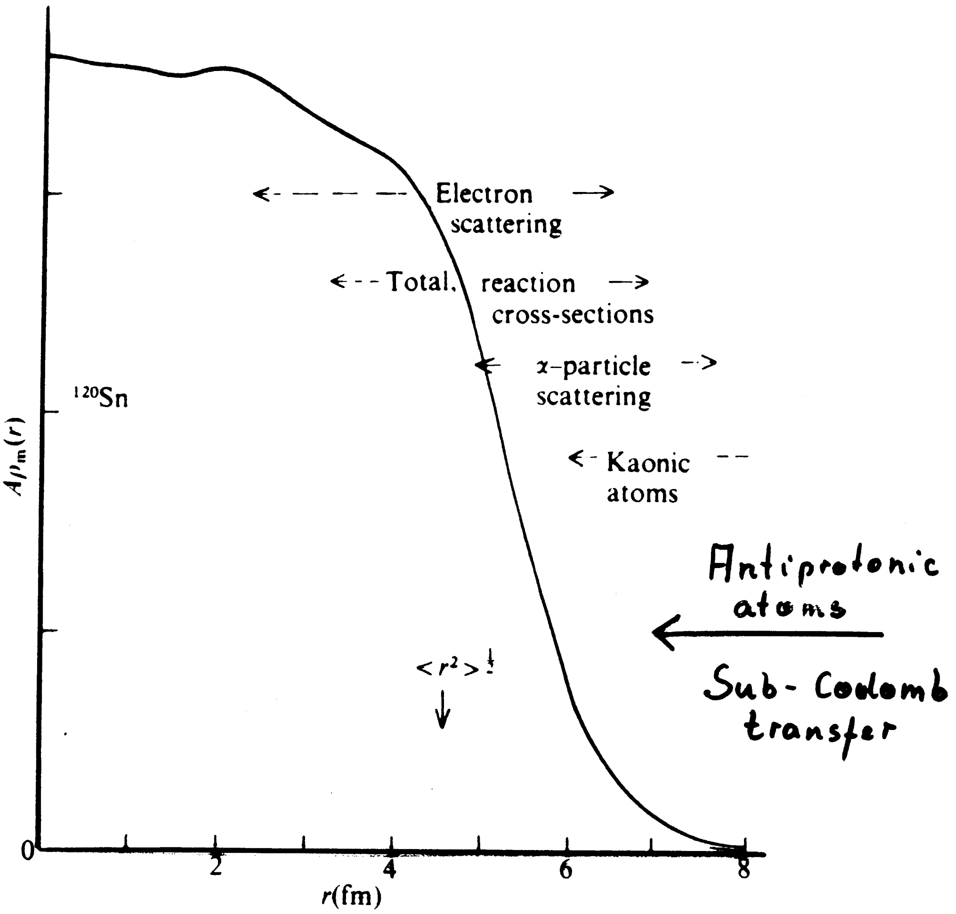

FIG. 11.1. **The nuclear matter distribution** $A\rho_m(r)$ **for** ^{120}Sn given by the BG (proton) **and ZD (neutron) distributions shown** in Fig. 2.2. **The horizontal lines show the region of the nucleus probed** by various **processes;** where the lines are broken the extent of the region is still uncertain. **(From Jackson 1975.)**

R.C. Barrett, D.F. Jackson

Nuclear Sizes and Structure

(1977)

Sub-Coulomb Pick-up on ^{208}Pb

(d,t) (p,d)

H.J. Körner and J.P. Schiffer

Phys. Rev. Lett. 27 (1971) 1457

- determined for a number of bombarding energies and angles

6 → $|\chi|^2$ values of neutron hole states

$3p_{1/2}$, $3p_{3/2}$, $2f_{5/2}$ ...

at 15 fm

- Saxon-Woods potential shape assumed

$$\rho_n(r) = \sum_i |\chi_i|^2$$

$\rho_p(R)$ → Sax. W. parameters adjusted to fit $\langle r^2 \rangle$ measured for the charge distribution

Sub-Coulomb Pickup on ^{208}Pb

(d,t) (p,d)

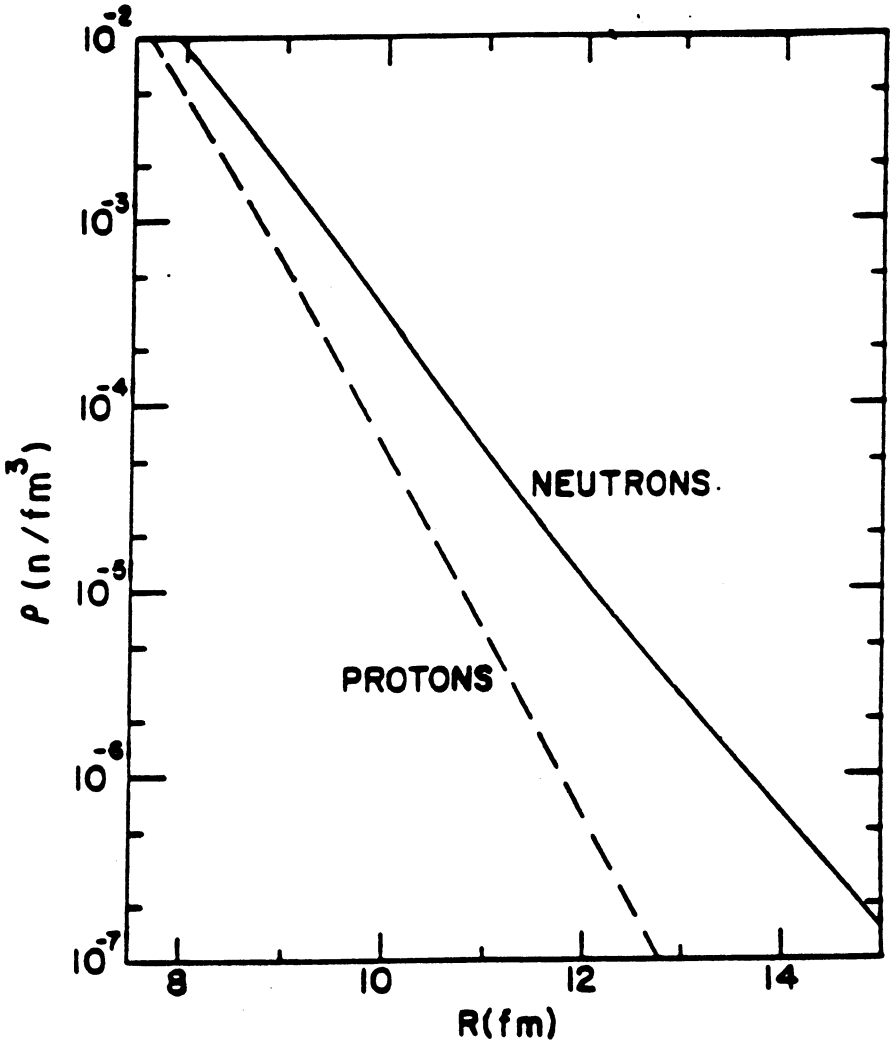

FIG. 1. Neutron and proton densities, derived as described in the text.

H. J. Körner and J. P. Schiffer

Phys. Rev. Lett. 27 (1971) 1457

$\bar{p}$

W. M. Bugg et al. Phys. Rev. Lett. 31 (1973) 475

BNL 30" hydrogen bubble chamber

stopped $\bar{p}$ on C, Ti, Ta, Pb

total charge of mesonic prongs investig.

$\bar{p}p$ net charge: 0

$\bar{p}n$ −1

$$f_{halo} = \frac{N(\bar{p}n)}{N(\bar{p}p)} \frac{Z_t}{N_t} \frac{\mathrm{Im}\, a_p}{\mathrm{Im}\, a_n}$$

^{12}C $\qquad$ ^{208}Pb

$f \underset{\text{ex def}}{=} 1.0$ $\qquad$ $f = 2.3 \pm 0.5$

multiple corrections necessary

K^-

D. H. Wilkinson Phil. Mag. 4 (1959) 215

D. H. Davis et al. N. Phys. B1 (1967) 435

E. H. Burhop N. Phys. B1 (1967) 43

Nuclear emulsions

Similar principle as anitprotonic experiment of Bugg

$$K^- + p \rightarrow \Sigma^{\mp} \pi^{\pm}$$

$$K^- + n \rightarrow \Sigma^- (\pi^0)$$

A. Bohr, B. R. Mottelson

Nuclear Structure

"In heavy nuclei, because of the Coulomb forces and associated neutron excess, there may be some difference between the density distributions of neutrons and protons. <u>Tentative</u> evidence bearing on this interesting problem is discussed ..."

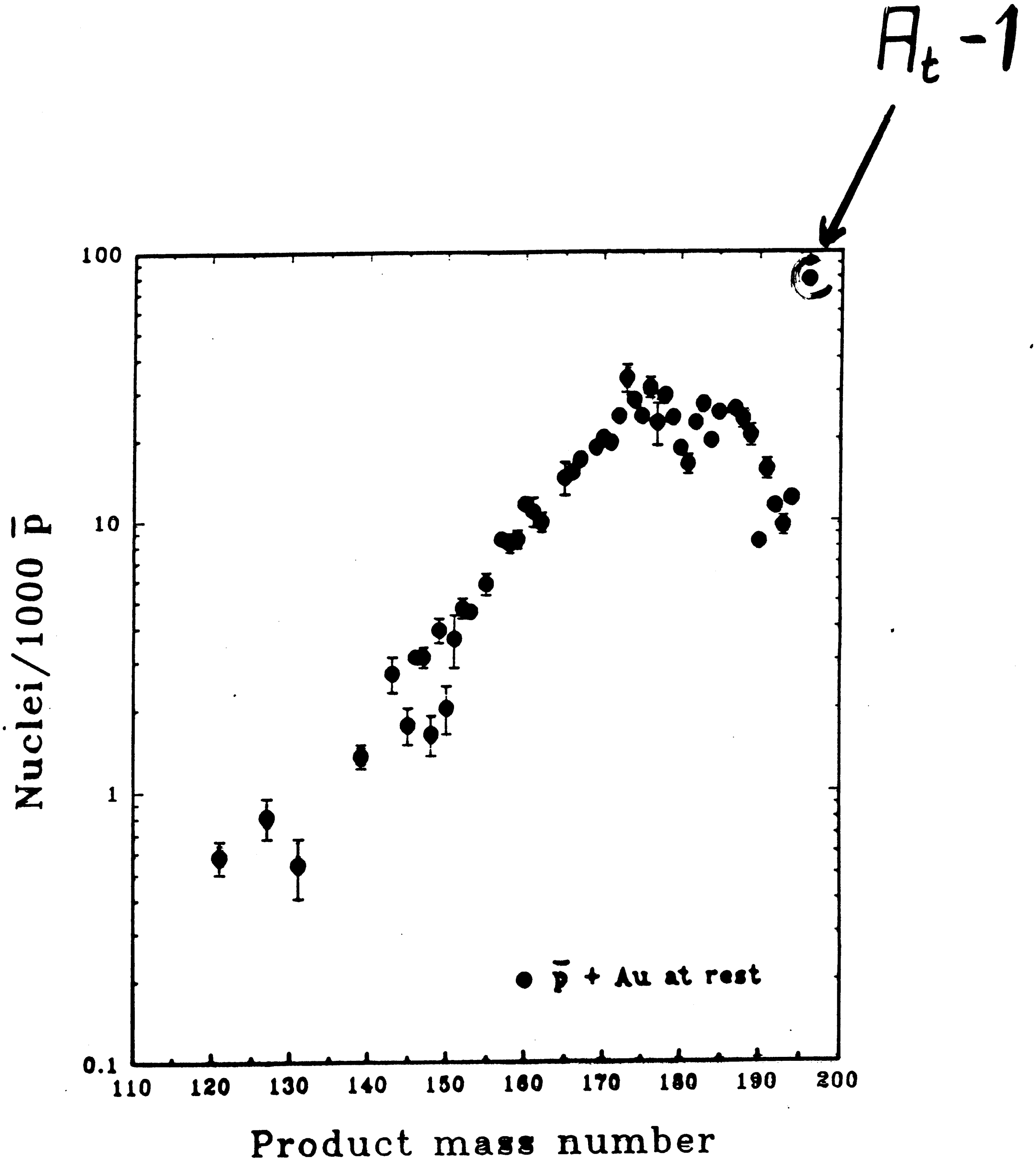
A_t -1
100
10
1
0.1
Nuclei/1000 p̄
110 120 130 140 150 160 170 180 190 200
Product mass number
p̄ + Au at rest

PS 203

Physics of the phenomenon of $A_{target} - 1$ production : <u>void cascade events</u>

- Close annihilations:

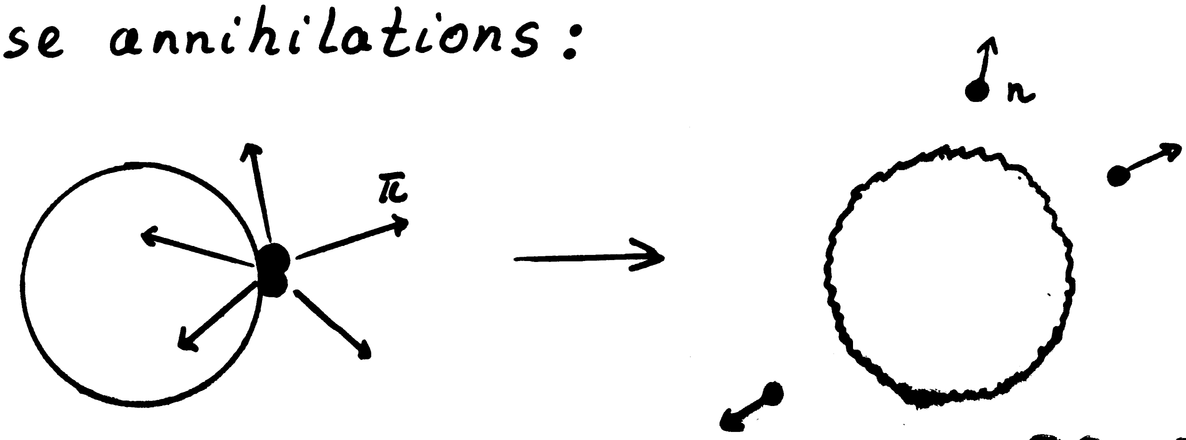

HOT PRODUCT

- Distant annihilations:

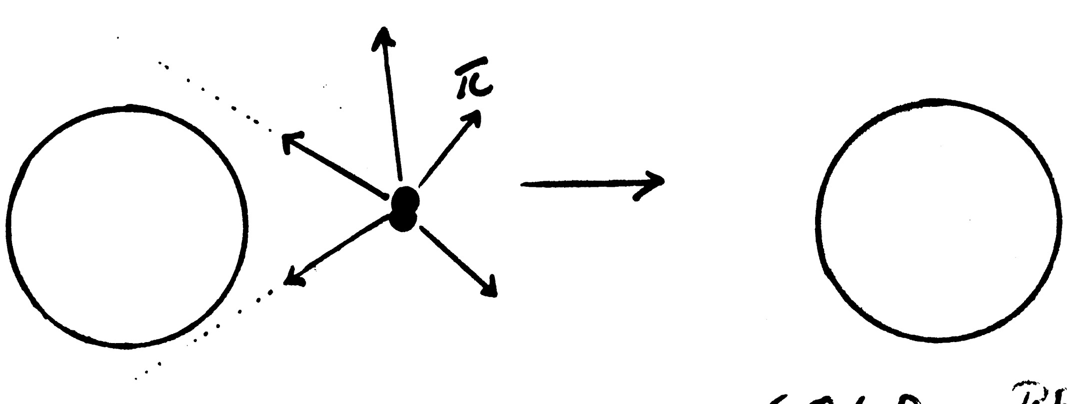

COLD PRODUCT

If, in a distant annihilation $\bar{p}$ encounters a neutron :

produced nucleus is $N_t - 1$

- encounters a proton :

produced nucleus is $Z_t - 1$

if $(N_t - 1)$ and $(Z_t - 1)$ products are both radioactive their yield can be determined by the radiochemical methods.

- The ratio of their yields :

$$\frac{Y(N_t - 1)}{Y(Z_t - 1)} = f\left(\frac{\rho_n}{\rho_p}\right)$$

for r where $P_{miss} \neq 0$

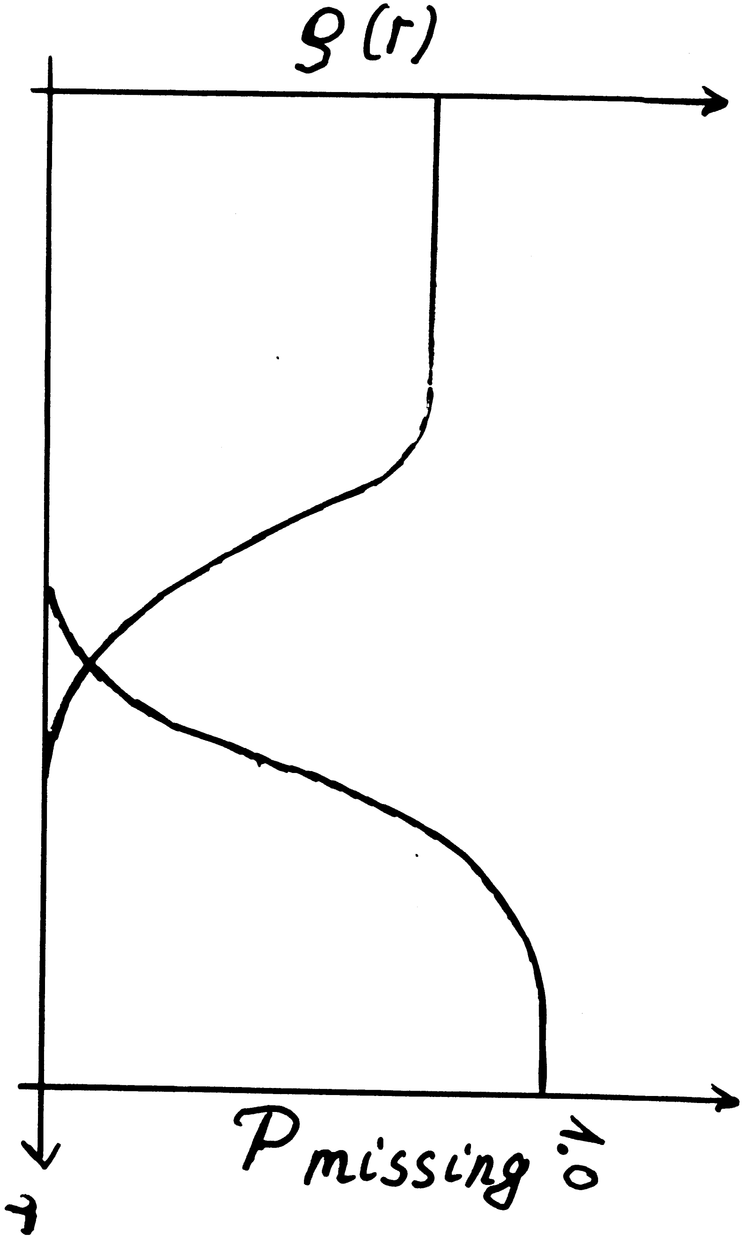

g(r)
P missing
1.0
r

U 232 70.0 a α 5.320; 5.263... sf γ (58 129...), e⁻ σ 73.1, σf 75.2	U 233 1.592 · 10⁵ a α 4.824; 4.783... γ (42; 97...) e⁻ σ 47.7; σf 531.1	U 234 0.005 2.446 · 10⁵ a α 4.775 4.723 γ (53 121 ...) e⁻ σ 100.2, σf < 0.65	U 235 0.720 [illegible]	U 236 2.342 · 10⁷ a [illegible]	U 237 6.75 d β⁻ 0.2... γ 60; 208... e⁻ σ 411; σf < 0.35	U 238 99.275 [illegible]
Pa 231 3.276 · 10⁴ a α 5.014 4.952 5.028 γ 27 303 300 e⁻ σ 210 σf 0.010	Pa 232 1.31 d β⁻ 0.3; 1.3 γ 969; 894 150 e⁻ σ 700 σf 700	Pa 233 27.0 d β⁻ 0.3; 0.6 γ 312; 300 341 e⁻ σ 21 + 20 σf < 0.1	Pa 234 1.17 m 6.70 h [illegible]	Pa 235 24.2 m β⁻ 1.4 .. γ 128-659	Pa 236 9.1 m β⁻ 2.0; 3.1... γ 642; 687; 1763... [illegible]	Pa 237 8.7 m β⁻ 1.4; 2.3... γ 854; 865 529; 541..
Th 230 7.54 · 10⁴ a α 4.688 4.621 γ 68 144 e⁻ σ 23.2 σf 0.0012	Th 231 25.5 h β⁻ 0.3; 0.4... γ 26; 84 e⁻	Th 232 100 1.405 · 10¹⁰ a α 4.013 3.954 sf γ (59) e⁻ σ 7.40 σf 0.000003	Th 233 22.3 m β⁻ 1.2 γ 87 29 459 e⁻ σ 1500 σf 15	Th 234 24.10 d β⁻ 0.2 .. γ 92; 63; e⁻ m σ 1.8 σf < 0.01	Th 235 6.9 m β⁻ γ 416-932	Th 236 37.1 m β⁻ 1.0 ... γ 111 113
Ac 229 62.7 m β⁻ 1.1 γ 165 569 262 146 135	Ac 230 122 s β⁻ 2.7. γ 455 508 1244 e⁻	Ac 231 7.5 m β⁻ γ 282; 307 221 186 369	Ac 232 35 s			

140 142 144 146

$$f_{halo}^{peripheral} = \frac{N(\bar{p}n)}{N(\bar{p}p)} \frac{Im\, a_p}{Im\, a_n} \frac{Z_t}{N_t}.$$

$$\frac{1}{(0.63)}$$

Halo factor

expresses the (normalized) ratio of antiproton encounters with neutrons to encounters with protons in the orbitals from which absorption takes place

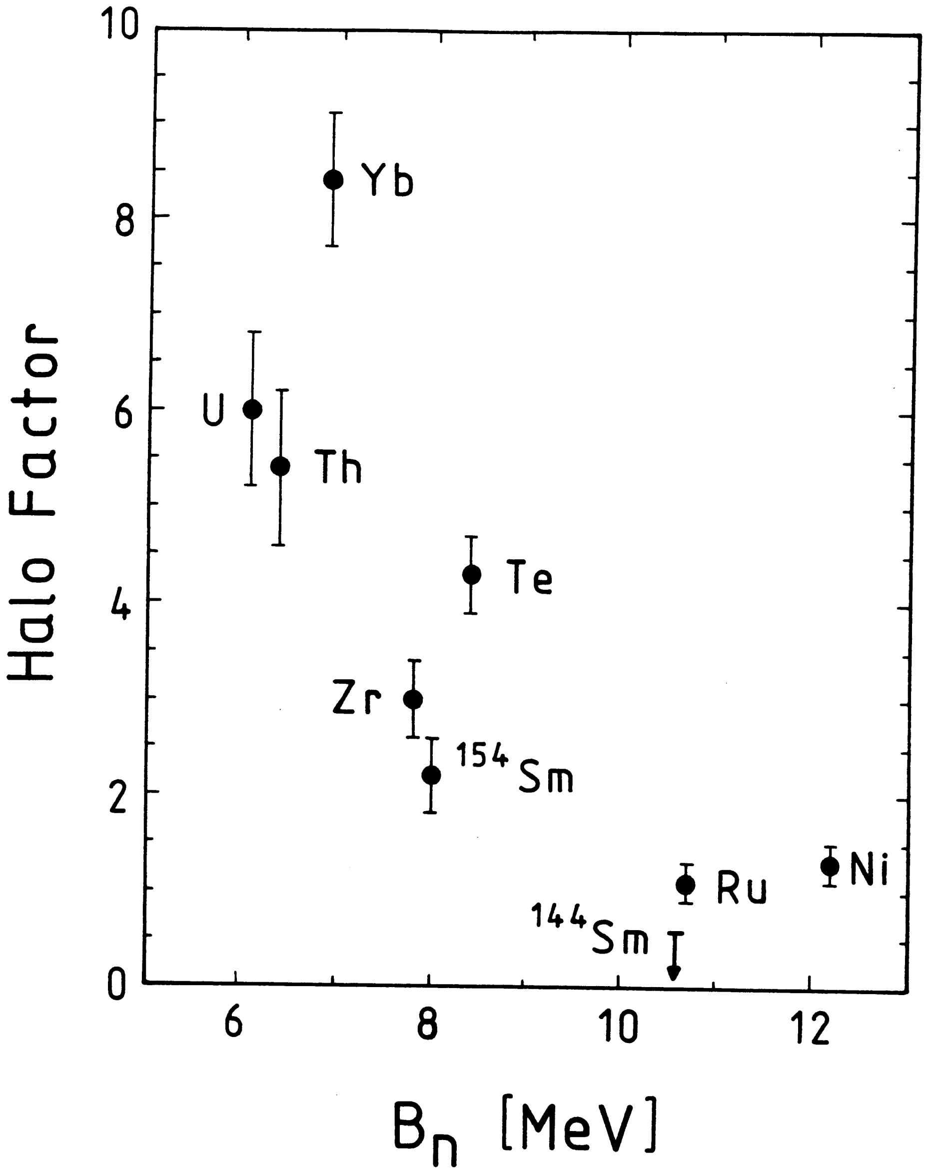

Halo Factor
10
8
6
4
2
0
6
8
10
12
B_n [MeV]
Yb
U
Th
Te
Zr
154Sm
Ru
Ni
144Sm

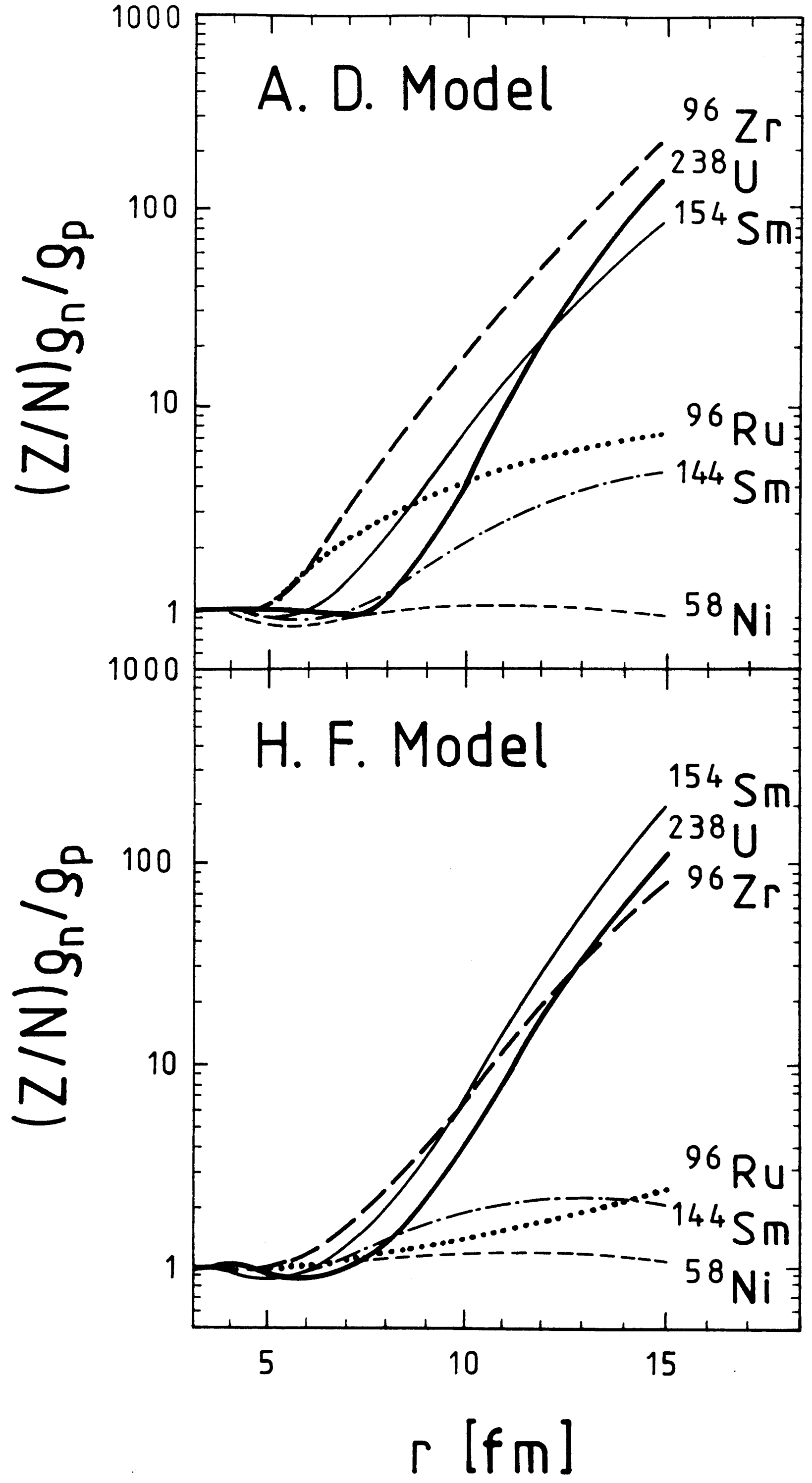
A. D. Model
H. F. Model
(Z/N)ρn/ρp
1000
100
10
1
96Zr
238U
154Sm
96Ru
144Sm
58Ni
5
10
15
r [fm]

THE PHYSICAL REVIEW
AND
PHYSICAL REVIEW LETTERS
1 Research Road - Box 1000
Ridge, New York 11961
Telephone (516) 924-5533

REQUEST FOR FACSIMILE SERVICE

DATE 19 October 1994 FAX # 011-48-2-659-2714

OF PAGES INCLUDING COVER 2 (CTA

TO: Dr. Jersy Jastrzebski AT: Warsaw University

DEPT: Heavy Ion Laboratory PHONE # 22-222-123

FROM: Physical Review Letters MS. CODE #: LW5096

TITLE: Neutron halo in heavy ...

AUTHORS: P. Lubinski et al.

Dear Dr. Jastrzebski:

The above manuscript has been accepted for publication in Physical Review Letters; there are no reviewer comments to address. The paper is now being prepared for the printer. Note that proofs are NOT sent. If any questions arise in the production process we will attempt to contact you.

Thank you for your cooperation.

Sincerely,

Editors
Physical Review Letters

AMERICAN PHYSICAL SOCIETY EDITORIAL OFFICE FAX # 516-924-5294

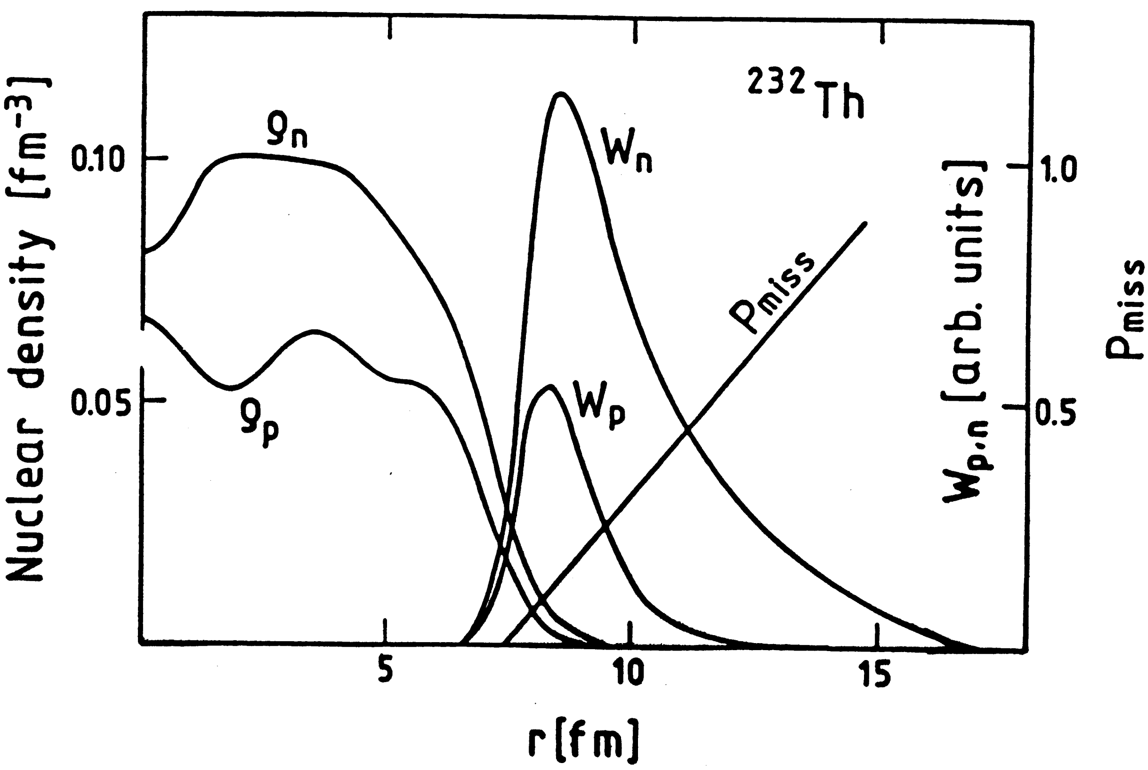

Figure 5. Neutron and proton densities, ρ_n and ρ_p (see also Fig. 3), the anti... absorption probability on neutrons, W_n, and on protons, W_p, and the "missing probabi... P_{miss} (from Ref. 27, see also text).

$$\frac{\Gamma}{2} = \int W(r)\, dr = \int Im\, V(r)\, |\chi_{n,\ell}(r)|^2\, r^2\, dr$$

$$V(r) = \frac{2\pi}{\mu}\, a\, \rho(r)$$

$$a = (1.53 \pm 0.27) + i\,(2.50 \pm 0.25)\ fm$$

(fit to light nuclei X-ray data)

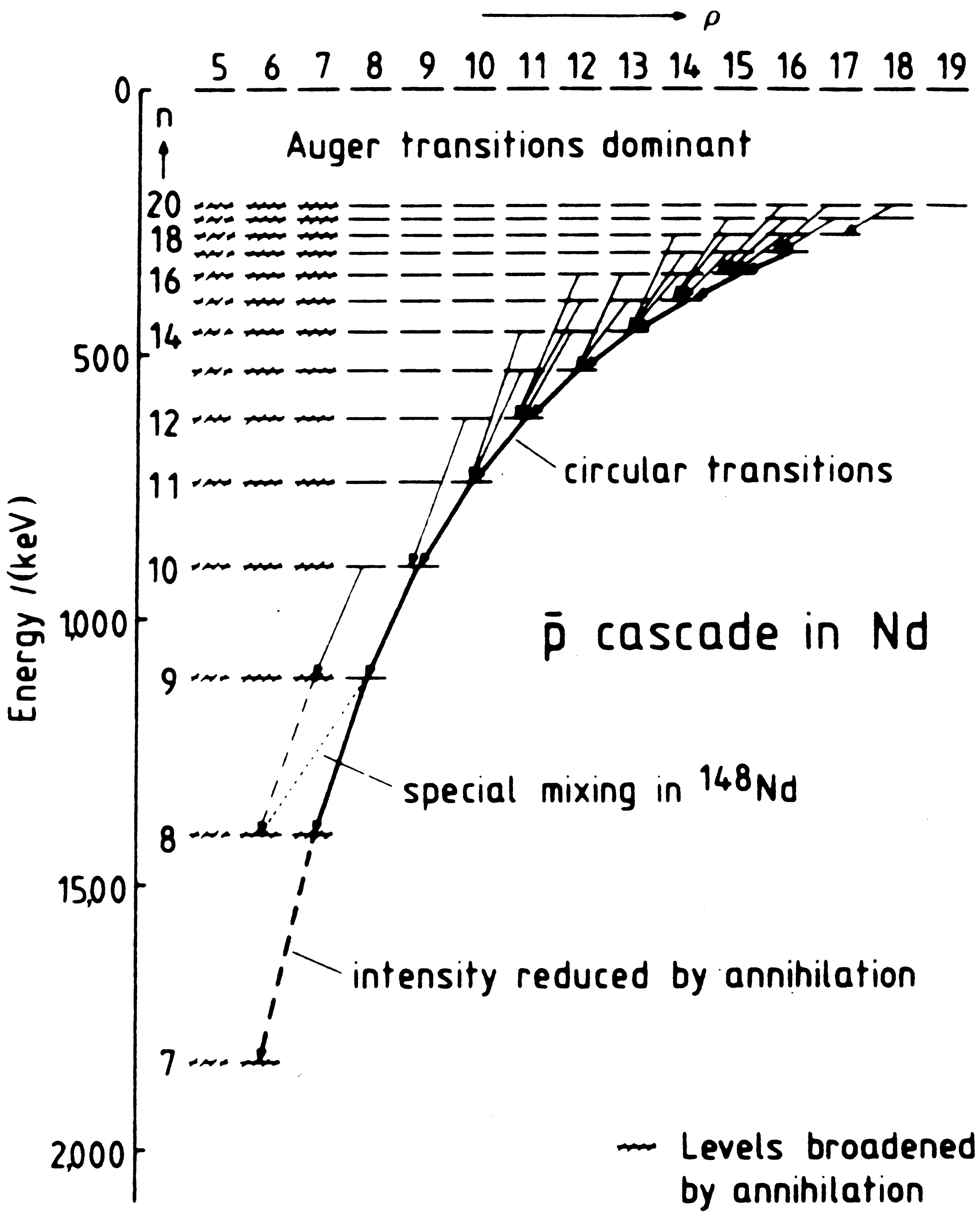

Antiprotonic levels in the Nd atom.

Fine structure splitting:

$$\Delta E_{n,l} = (g_0 + 2g_1)\frac{(\alpha Z)^4}{2n^3}\frac{\mu}{l(l+1)}$$

g_0 - Dirac $= -1$

g_1 - anomalous g factor (Pauli)

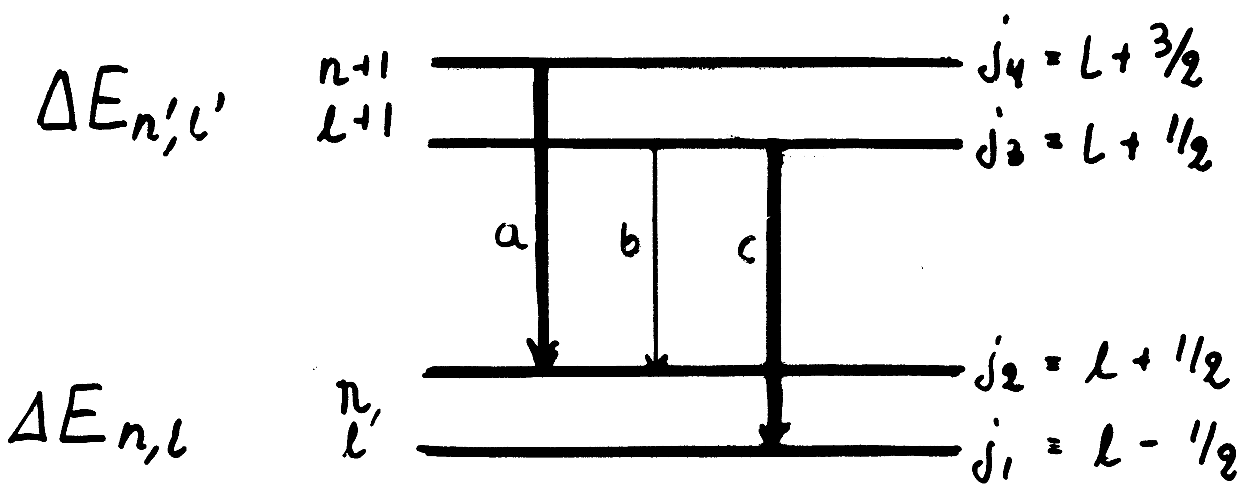

Lower level structure

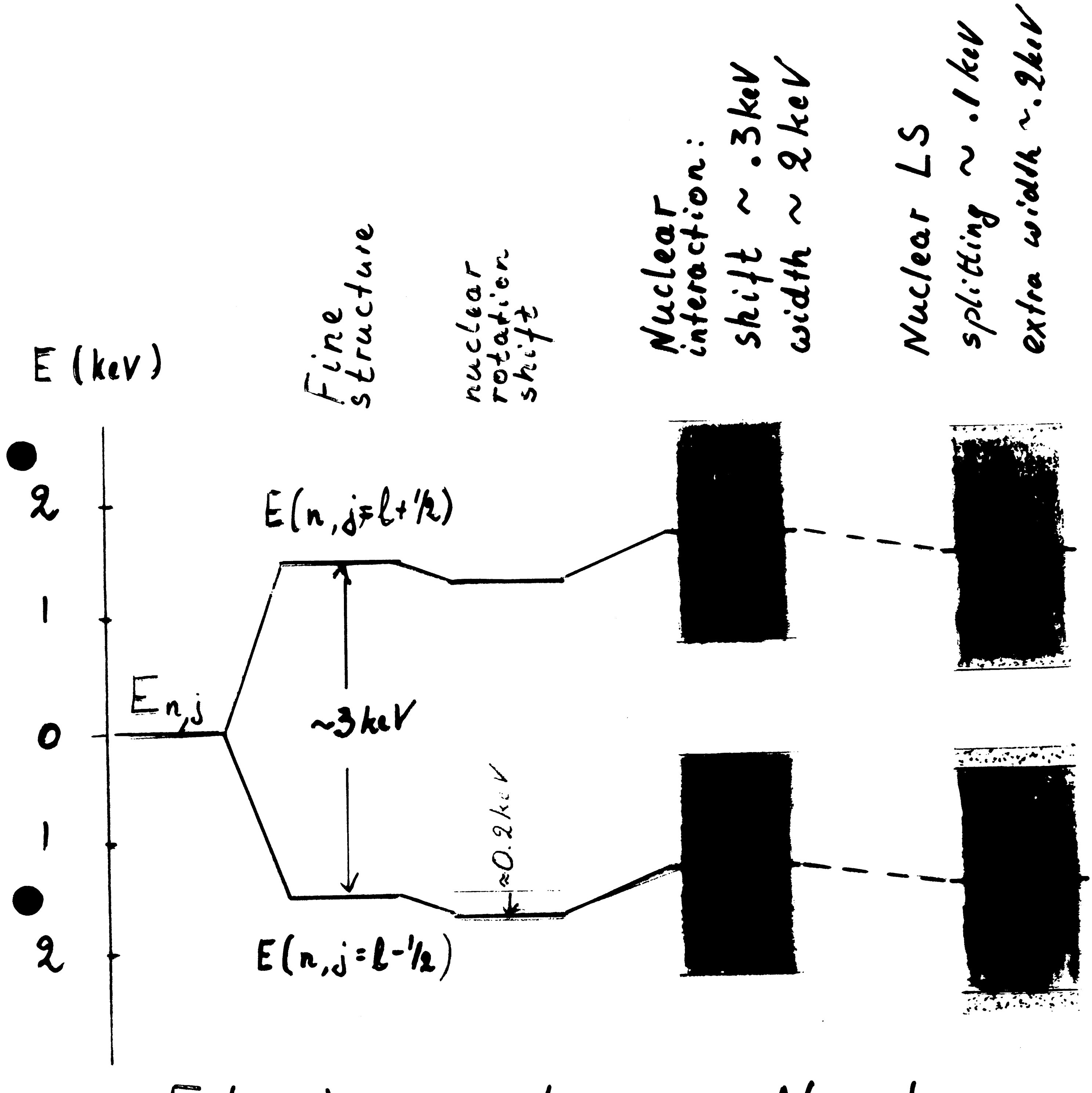

Electromagnetic-
calculable

Nuclear-
to measure

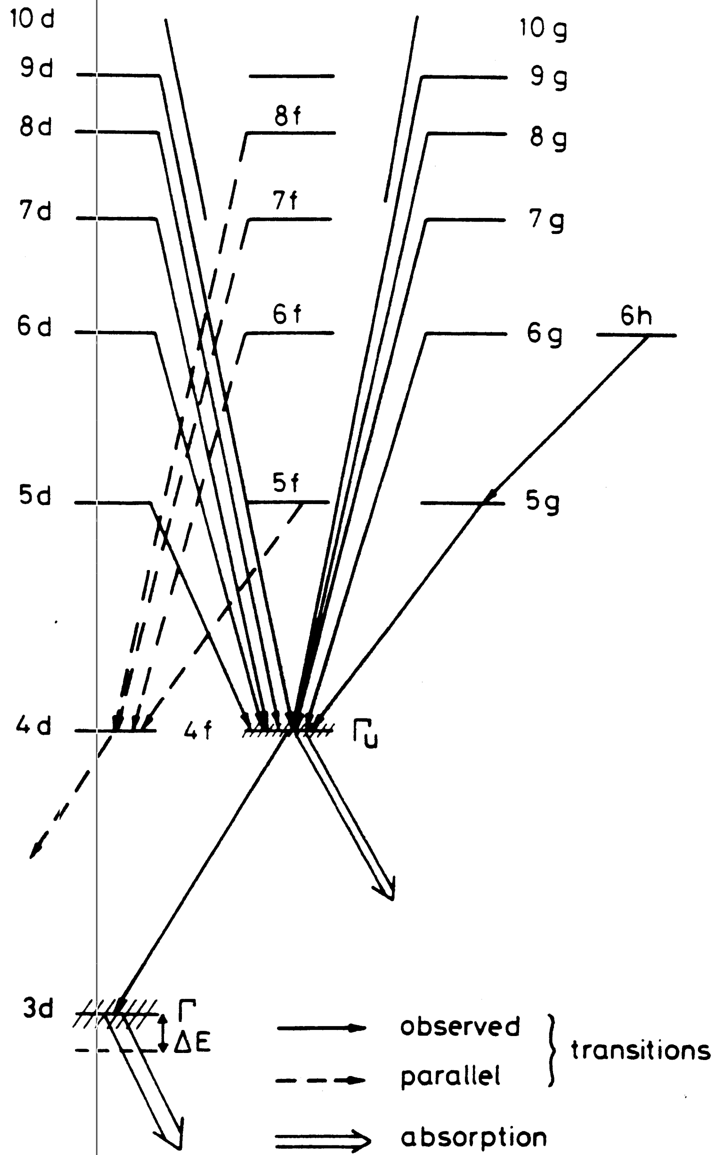

Fig. 1. Antiprotonic atom level scheme showing how the width (Γ_u) of the upper level can be determined.

Observables of the proposed experiment:

Lower level shift	ε
Lower level width	Γ_{low}
Upper lever width	Γ_{up}
Absolute transition intensities	I_x

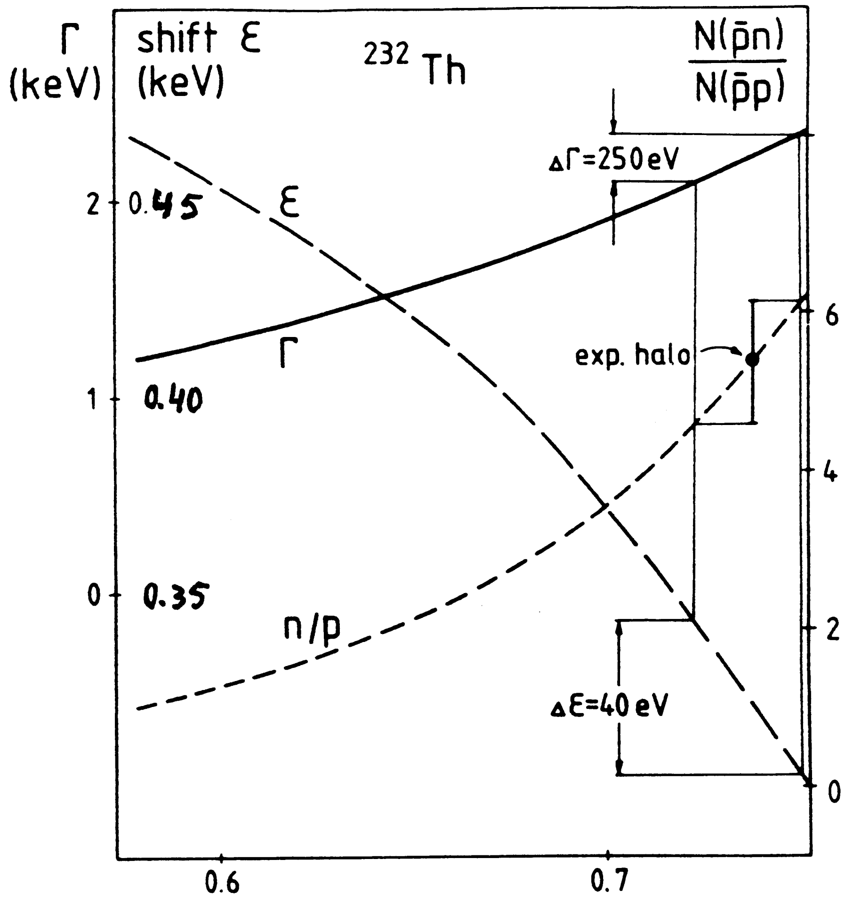

Neutron surface parameter a_n [fm]

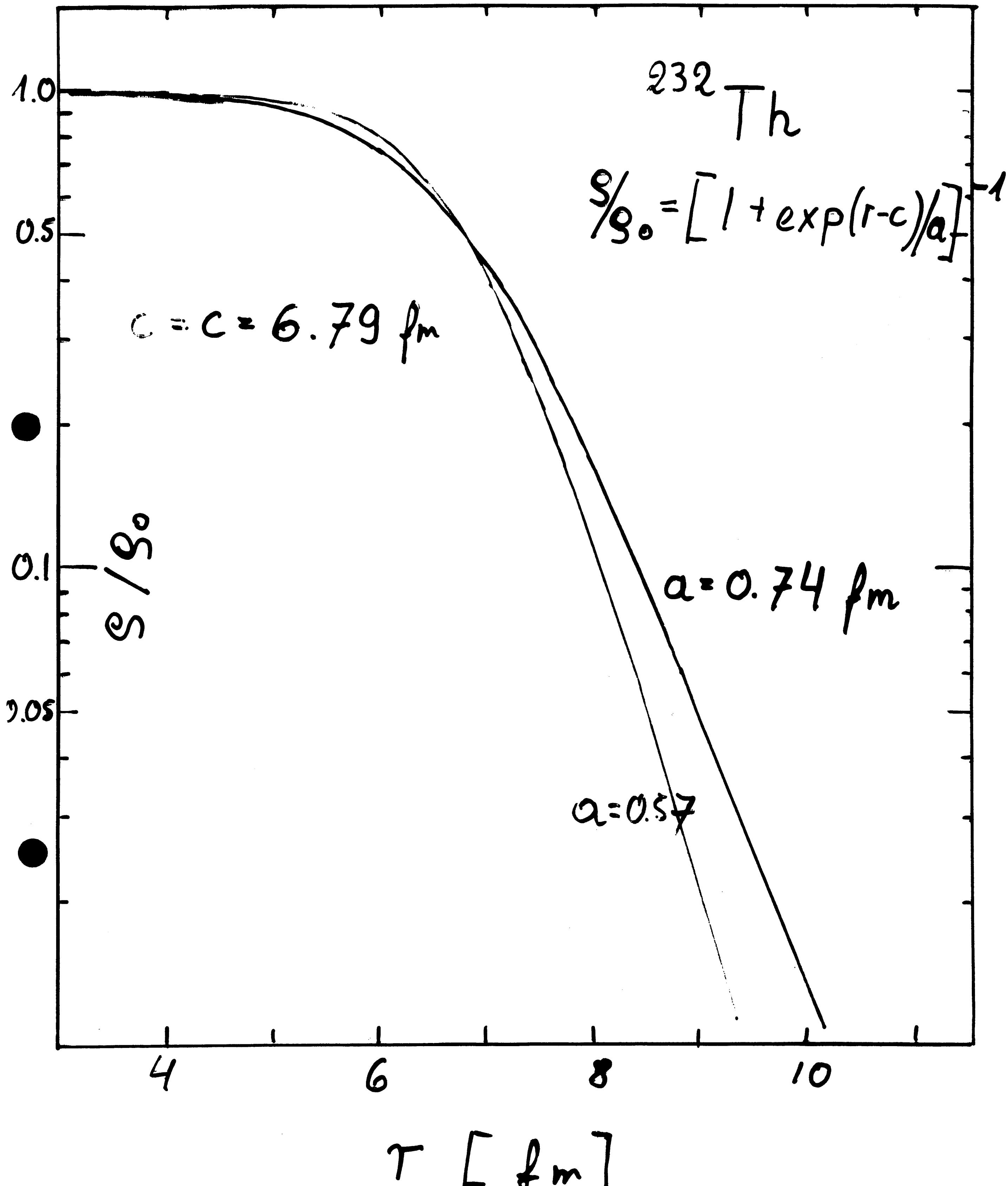

^{232}Th
ϱ/ϱ₀ = [1 + exp(r-c)/a]$^{-1}$
c = c = 6.79 fm
a = 0.74 fm
a = 0.57
1.0
0.5
0.1
0.05
ϱ/ϱ₀
4
6
8
10
r [fm]

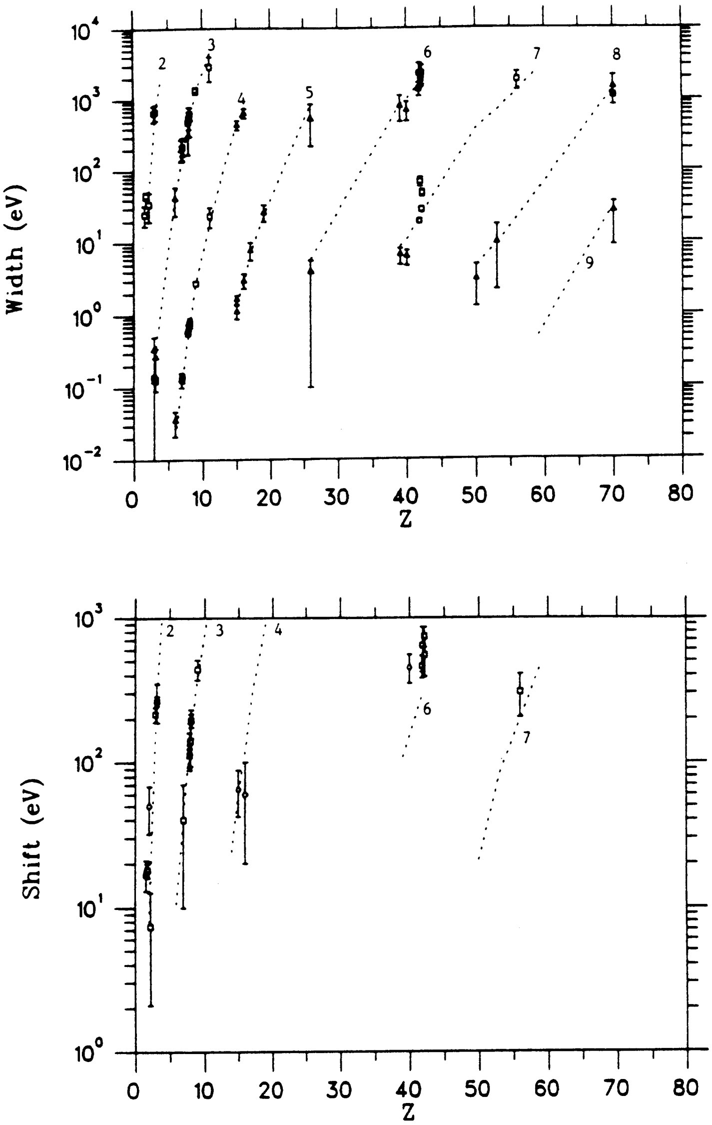

Fig. 4. Measured shifts (with reversed sign) and widths for $\bar{p}$-atoms. The dashed curve shows values calculated using the simple optical model (eq. (5)) with $\bar{a}$ = 1.53 + i2.50 fm.

Batty, 1990

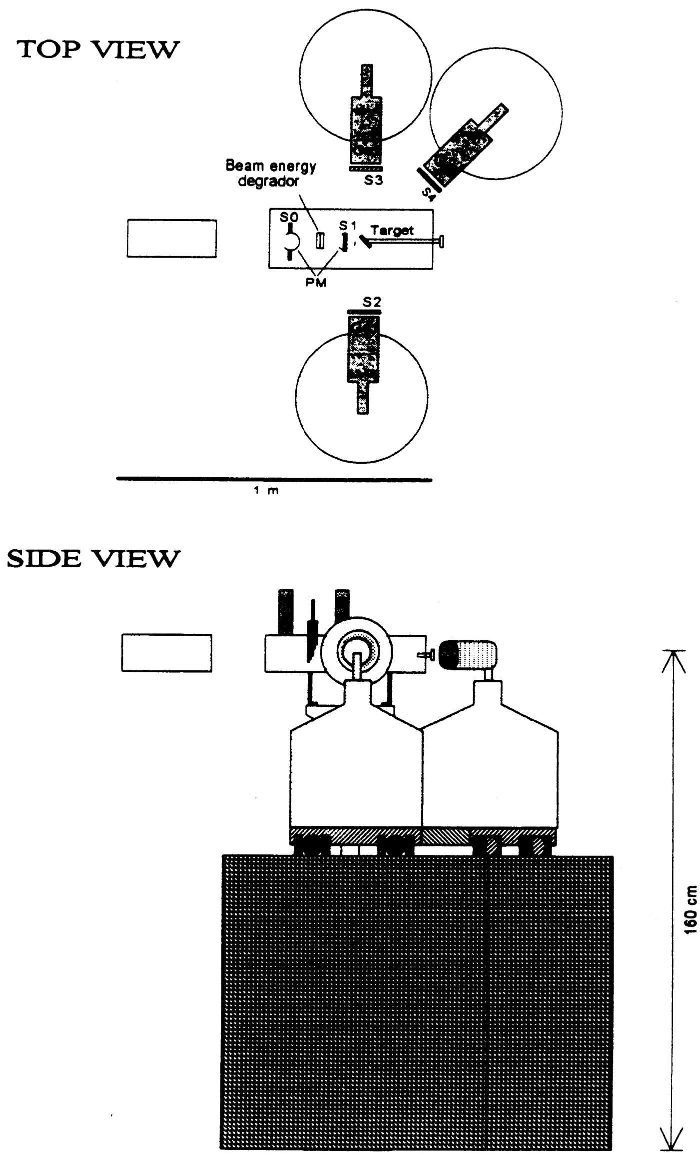

Fig. 6. The general view of the main parts of the experimental setup.

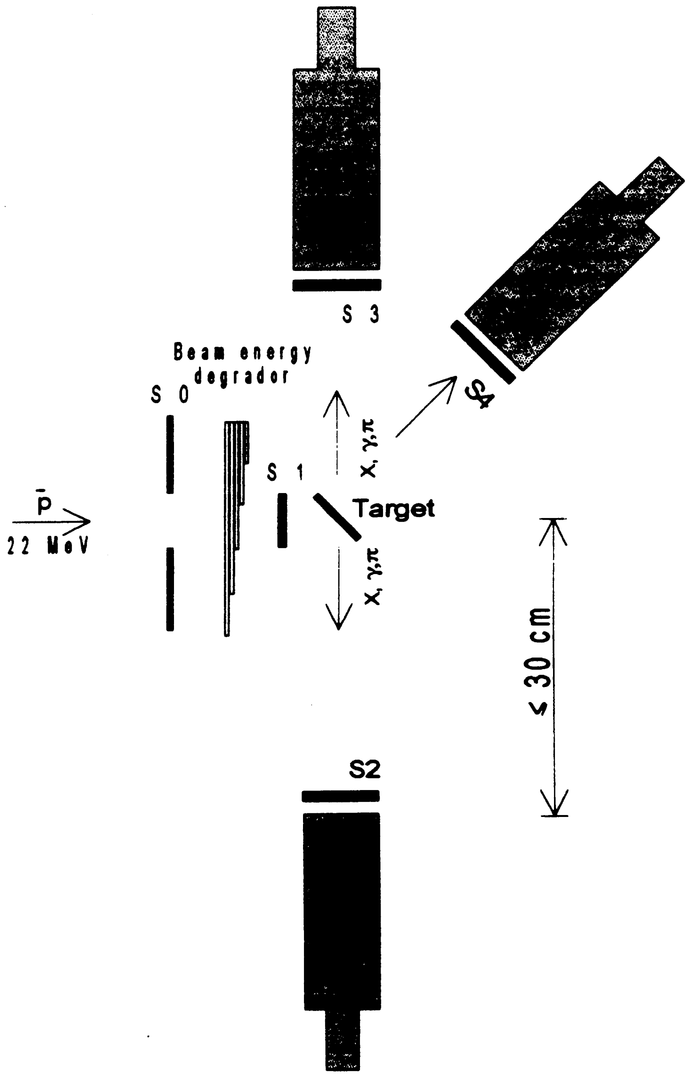

Fig. 7. The schematic view of the target - counter ensemble.

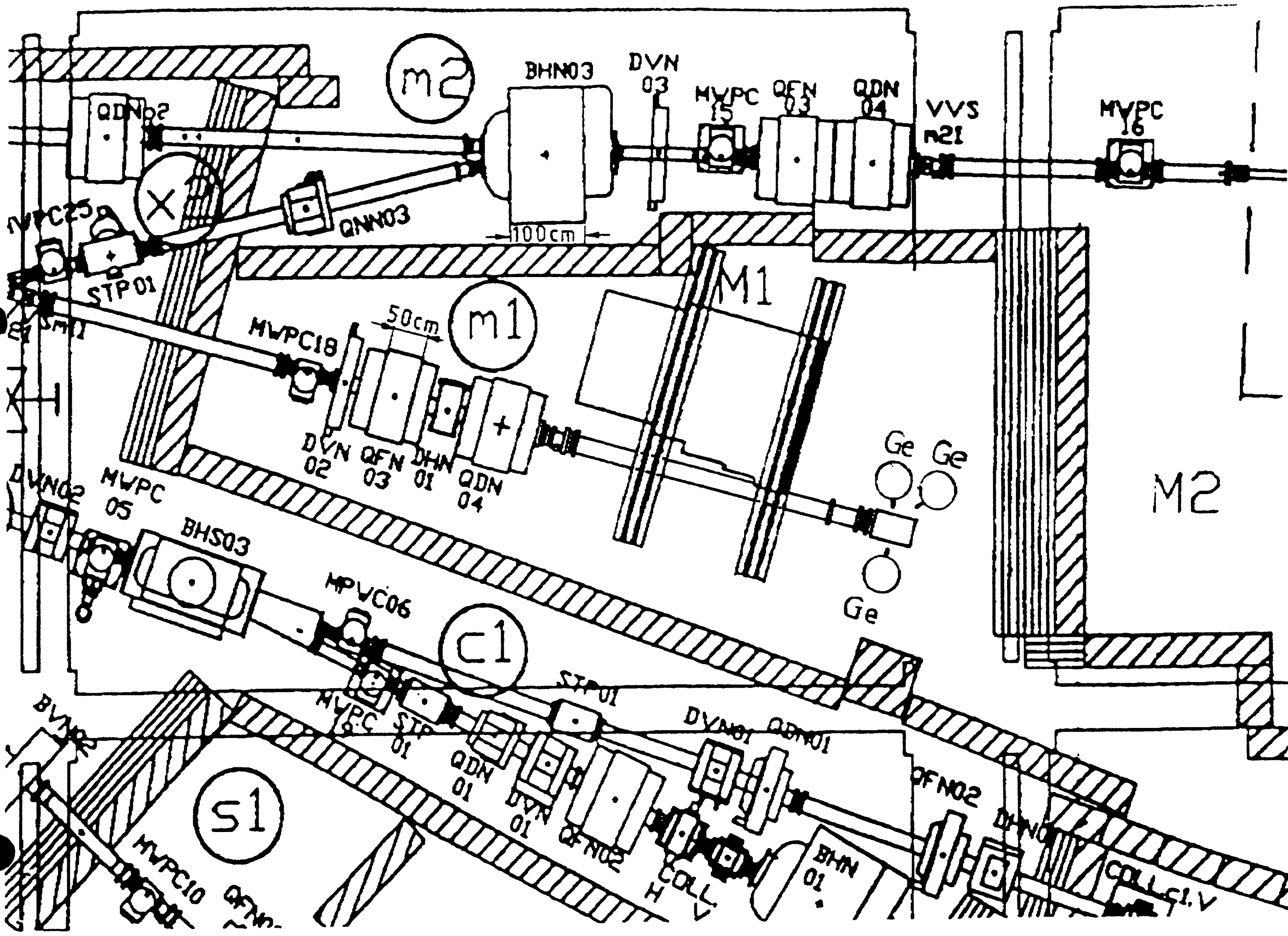
m2
BHN03
DVN
03
MWPC
15
QFN
03
QDN
04
VVS
m21
MWPC
16
QDN02
QNN03
MWPC25
STP01
100cm
M1
m1
50cm
MWPC18
DVN
02
QFN
03
DHN
01
QDN
04
Ge
Ge
Ge
M2
DVN02
MWPC
05
BHS03
MPWC06
c1
STP01
MWPC
STP
01
QDN
01
DVN01
QDN01
DVN
01
QFN02
QFN02
COLL.
H
V
BHN
01
s1
MWPC10
COLL.c1.V

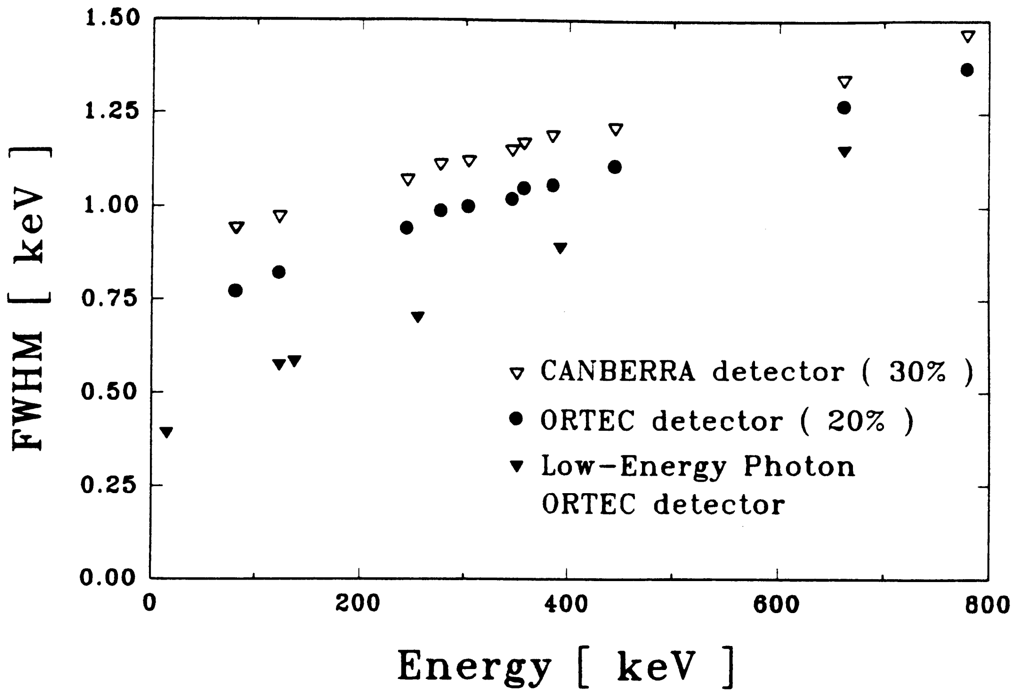

Fig. 11. Photo-peak resolution (FWHM) as a function of the gamma-ray energy for three available detectors.

The following table compares the estimate for gamma-X ORTEC and Low-Energy Photon ORTEC detectors previously described:

	Gamma-X ORTEC detector (Distance 30 cm)	Low-Energy Photon ORTEC detector (Distance 10 cm)
Detector surface	1892 mm^2	491 mm^2
Detector thickness	49 mm	13 mm
Solid angle (% 4Π)	0.16	0.34
γ-ray efficiency (200 keV)	1.0	0.8
π efficiency	1	1
p efficiency	1	1
π energy loss (E_π = 200 MeV)	37 MeV	10 MeV
p energy loss (E_p = 50 MeV)	50 MeV	50 MeV
counting rates (10^5 $\bar{p}$ stopped in the target)		
X-rays	1860/sec	2860/sec
π	400/sec	850/sec
p	160/sec	340/sec
Energy deposition rate	23 000 MeV/sec	25 000 MeV/sec
Preamplifier rate limit (from producer)	140 000 MeV/sec	≈ 30 000 MeV/sec
γ Peak /Total ratio (200 keV)	0.55	0.32
Single photopeak counting rate	102/sec	92/sec

About 10^6 counts in a photopeak will be collected during 5 h of measuring time with 10^5 $\bar{p}$ps. Pions and charged particles will overload the X and γ-X detectors. For both detectors the recovery time will be comparable so the γ-X detector will perform better due to lower rate. However energy resolution is better for the X detector by about 25 %. Plastic scintilators in front of detectors will prevent triggering data acquisition during overload (anticoincidence).

Expected results

- Fix the atomic cascade and determine states of the nuclear capture in nuclei where the neutron halo was detected - precision of the annihilation site and absorption probability distribution

- From shifts and widths in a number of targets determine the phenomenological $\bar{p}$ Nucleus optical potential in heavy nuclei a_R, a_i, $(r_0)_R$, $(r_0)_i$

- Use the neutron halo information as a supplementary constraint on this potential.

OBSERVATION OF ANTIPROTONIC ATOMS

A. BAMBERGER, U. LYNEN, H. PIEKARZ *, J. PIEKARZ **, B. POVH and H. G. RITTER
Max-Planck-Institut für Kernphysik, Heidelberg, Germany
and CERN, Geneva, Switzerland

and

G. BACKENSTOSS, T. BUNACIU, J. EGGER ***, W. D. HAMILTON ‡ and H. KOCH
Institut für Experimentelle Kernphysik der Universität und des Kernforschungszentrums, Karlsruhe, Germany
and CERN, Geneva, Switzerland

Received 28 August 1970

X-rays originating from the antiprotonic cascade have been observed for several elements. From the energies of the measured antiprotonic transitions of $_{81}$Tl, the mass of the antiproton could be determined to be 938.3 ± 0.5 MeV. With this result the masses of the antiproton and the proton are equal within 0.5 MeV with a confidence of 68 %. The magnetic moment of the antiproton shows up in a broadening of the $n = 10 \rightarrow n = 9$ transition.

In this letter we report the first measurement of X-rays originating from the atomic transitions of antiprotons bound in a nuclear Coulomb field.

Antiprotons stopped in a target will finally be captured into Bohr orbits of the target nuclei. This capture is expected to take place into orbits with high main quantum numbers. Subsequently, the antiprotons will cascade down to lower orbits releasing their energy by emission of either Auger electrons or X-rays. For sufficiently low quantum numbers, the overlap between the atomic antiproton wave function and the nucleus becomes so large that nucelar absorption dominates the radiative processes and no further X-rays are observed. According to perturbation calculations for nuclei in the oxygen region, the cascade is expected to terminate with the transition $n = 4 \rightarrow n = 3$ at about 70 keV, whereas in heavy nuclei such as lead the transition $n = 9 \rightarrow n = 8$ with an energy of 550 keV should be the last with a strongly reduced yield. The energies of these X-rays can be well calculated because the nuclear interaction is important only for the lowest populated levels.

* On leave of absence from: Institute of Nuclear Research, Warsaw, Poland.
** On leave of absence from: Institute of Experimental Physics, University of Warsaw, Warsaw, Poland.
*** Visitor from ETH Zürich, Switzerland.
‡ Present address: University of Sussex, Brighton, England.

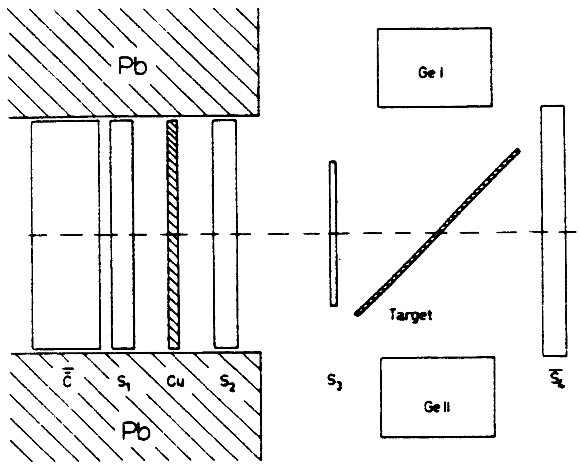

Fig. 1. Experimental set-up of the beam telescope, the target and two Ge(Li)-detectors.

A low momentum separated beam has been constructed at the CERN Proton Synchrotron for experiments with stopped particles [1]. In this beam about 300 antiprotons can be stopped in a 4 g/cm^2 thick target with 7×10^{11} protons hitting the 6 cm long tungsten production target of the slow ejection. The antiproton beam is strongly contaminated with 10^3 passing pions per stopped antiproton. A careful identification of the antiprotons is made with the beam tele-